



Biodegradation of 3-Chloronitrobenzene and 3-Bromonitrobenzene by *Diaphorobacter* sp. Strain JS3051

Zhi-Jing Xu,^a Jim C. Spain,^b  Ning-Yi Zhou,^a  Tao Li^a

^aState Key Laboratory of Microbial Metabolism, Joint International Research Laboratory of Metabolic and Developmental Sciences, and School of Life Sciences and Biotechnology, Shanghai Jiao Tong University, Shanghai, China

^bCenter for Environmental Diagnostics & Bioremediation, University of West Florida, Pensacola, Florida, USA

ABSTRACT Halonitrobenzenes are toxic chemical intermediates used widely for industrial synthesis of dyes and pesticides. Bacteria able to degrade 2- and 4-chloronitrobenzene have been isolated and characterized; in contrast, no natural isolate has been reported to degrade *meta*-halonitrobenzenes. In this study, *Diaphorobacter* sp. strain JS3051, previously reported to degrade 2,3-dichloronitrobenzene, grew readily on 3-chloronitrobenzene and 3-bromonitrobenzene, but not on 3-fluoronitrobenzene, as sole sources of carbon, nitrogen, and energy. A Rieske nonheme iron dioxygenase (DcbAaAbAcAd) catalyzed the dihydroxylation of 3-chloronitrobenzene and 3-bromonitrobenzene, resulting in the regiospecific production of ring-cleavage intermediates 4-chlorocatechol and 4-bromocatechol. The lower activity and relaxed regiospecificity of DcbAaAbAcAd toward 3-fluoronitrobenzene is likely due to the higher electronegativity of the fluorine atom, which hinders it from interacting with E204 residue at the active site. DccA, a chlorocatechol 1,2-dioxygenase, converts 4-chlorocatechol and 4-bromocatechol into the corresponding halomuconic acids with high catalytic efficiency, but with much lower K_{cat}/K_m values for fluorocatechol analogues. The results indicate that the Dcb and Dcc enzymes of *Diaphorobacter* sp. strain JS3051 can catalyze the degradation of 3-chloro- and 3-bromonitrobenzene in addition to 2,3-dichloronitrobenzene. The ability to utilize multiple substrates would provide a strong selective advantage in a habitat contaminated with mixtures of chloronitrobenzenes.

IMPORTANCE Halonitroaromatic compounds are persistent environmental contaminants, and some of them have been demonstrated to be degraded by bacteria. Natural isolates that degrade 3-chloronitrobenzene and 3-bromonitrobenzene have not been reported. In this study, we report that *Diaphorobacter* sp. strain JS3051 can degrade 2,3-dichloronitrobenzene, 3-chloronitrobenzene, and 3-bromonitrobenzene using the same catabolic pathway, whereas it is unable to grow on 3-fluoronitrobenzene. Based on biochemical analyses, it can be concluded that the initial dioxygenase and lower pathway enzymes are inefficient for 3-fluoronitrobenzene and even misroute the intermediates, which is likely responsible for the failure to grow. These results advance our understanding of how the broad substrate specificities of catabolic enzymes allow bacteria to adapt to habitats with mixtures of xenobiotic contaminants.

KEYWORDS 3-chloronitrobenzene, *Diaphorobacter*, biodegradation, halonitrobenzene

Halonitrobenzenes (HNBs) are important intermediates in the manufacturing of pharmaceuticals, pesticides, dyes, and rubber-processing chemicals (1, 2). Extensive use of HNBs, especially chloronitrobenzenes, at chemical manufacturing sites as chemical intermediates has led to their release into the environment (3, 4). HNBs are toxic to aquatic organisms and also toxic to humans through inhalation, ingestion, or skin absorption (5). Therefore, it is desirable to develop effective means including bioremediation to remove them from contaminated water or soil.

Previous studies have described pure cultures capable of utilizing 2-chloronitrobenzene (2CNB) (6), 2-bromonitrobenzene (2BNB) (7), and 4-chloronitrobenzene (4CNB) (8), as well as

Editor Maia Kivisaar, University of Tartu

Copyright © 2022 American Society for Microbiology. All Rights Reserved.

Address correspondence to Tao Li, lisuitao@sjtu.edu.cn.

The authors declare no conflict of interest.

Received 14 December 2021

Accepted 19 February 2022

Published 28 March 2022

multi-substituted halonitrobenzenes including 2,3-dichloronitrobenzene (23DCNB) and 3,4-dichloronitrobenzene (34DCNB) (9) as sole carbon, nitrogen, and energy sources for growth. Various catabolic pathways are used by aerobic bacteria to carry out the initial steps in biodegradation of the halogenated and nitrated compounds. *Pseudomonas putida* strain ZWL73 and *Comamonas* sp. strain CNB-1 initiate catabolism of 4CNB by partial reduction of the nitro group (8, 10). In contrast, *Pseudomonas stutzeri* ZWLR2-1 (6), *Diaphorobacter* sp. strain JS3051, and *Diaphorobacter* sp. strain JS3050 (9) initiate 2CNB, 23DCNB, and 34DCNB degradation via oxidative reactions. These latter compounds are converted into chlorocatechols by ring-hydroxylating dioxygenases that are homologous to the naphthalene dioxygenase from *Ralstonia* sp. strain U2 (11–13). The resultant chlorocatechols are then assimilated through a modified *ortho*-cleavage pathway.

To date, there is no natural isolate reported to be capable of growth on any of *meta*-halonitrobenzenes. It was reported previously that 3CNB in wastewater was biodegraded in a membrane bioreactor by a mixed culture, but the bacteria responsible were not reported. Park et al. reported degradation of 3CNB by a coculture of *P. putida* HS12 and *Rhodococcus* sp. strain HS51 (14). The two strains synergistically metabolized the 3CNB through a partial reduction pathway when succinate was provided as a primary carbon source. Subsequently, a metabolically engineered strain of *Ralstonia* was constructed to degrade 3CNB via an oxidative pathway consisting of a nitroarene dioxygenase and chlorocatechol catabolic enzymes from different origins (15). The constructed strain clearly degraded 3CNB but with a relatively low growth rate, likely due to suboptimal regulation of the components of the catabolic pathway. Recently, we isolated *Diaphorobacter* sp. strain JS3050 and *Diaphorobacter* sp. strain 3051 from a chloronitrobenzenes contaminated site based on their abilities to grow on 3,4-dichloronitrobenzene and 2,3-dichloronitrobenzene (9). Subsequent investigation of the molecular basis for the degradation revealed that in both isolates the Rieske-iron dioxygenases that catalyze the initial denitration reactions had high activity toward 3-chloronitrobenzene (12, 13). The resultant 4-chlorocatechol was also a good substrate for the chlorocatechol dioxygenases that catalyzes the initial reaction in the downstream pathways that leads to assimilation of chlorocatechols. The findings led us to hypothesize that the isolates might grow on *meta*-halobenzenes. In this study, we thoroughly investigated the growth capacity of strain JS3051 on three *meta*-halonitrobenzenes. The strain grew readily on 3CNB and 3BNB, but not 3FNB. The activities of the initial dioxygenase and the ring-cleavage dioxygenase were also determined. The results provide several lines of evidence for explaining the growth capabilities of JS3051 on *meta*-HNBs and also reveal the potential of strain JS3051 for the degradation of multiple halonitrobenzenes found as mixtures in contaminated sites.

RESULTS

Growth of *Diaphorobacter* sp. strain JS3051 on 3CNB, 3BNB and 3FNB. Strain JS3051 was isolated originally based on its ability to grow on 23DCNB via an initial dioxygenation at C-1, 2 to form 3,4-dichlorocatechol catalyzed by a Rieske nonheme iron dioxygenase (DcbAaAbAcAd). The dioxygenase has surprisingly broad substrate specificity for other nitroarenes, especially for 3CNB (13). Thus, we decided to test whether strain JS3051 could grow on 3CNB. Strain JS3051 grew readily in MSM with 3CNB (doubling time 11.8 ± 0.7 h) as sole carbon and nitrogen resource accompanied by nitrite release (Fig. 1A). No UV-observable products were detected by high-performance liquid chromatography (HPLC) analysis. Strain JS3051 also grew well on 3-bromonitrobenzene (3BNB) (Fig. 1B) with a doubling time of 10.9 ± 0.5 h, but not on 3-fluoronitrobenzene (3FNB) (Fig. 1C) under the same conditions. No attempt was made to optimize growth conditions.

DcbAaAbAcAd catalyzed the dioxygenation of *meta*-HNBs. Previously, we identified DcbAaAbAcAd from strain JS3051 as a 2,3-dichloronitrobenzene dioxygenase with substantial activity toward 3CNB (13), but its activity toward 3BNB and 3FNB was not tested. We hypothesized that the failure of JS3051 to grow on 3FNB could be because 3FNB is a poor substrate for the dioxygenase. Therefore, whole-cell biotransformations of *meta*-HNBs were performed with *E. coli* cells carrying pETDuet-DCB, and the rate of nitrite release was taken as an indication of dioxygenase activity. The DcbAaAbAcAd shows

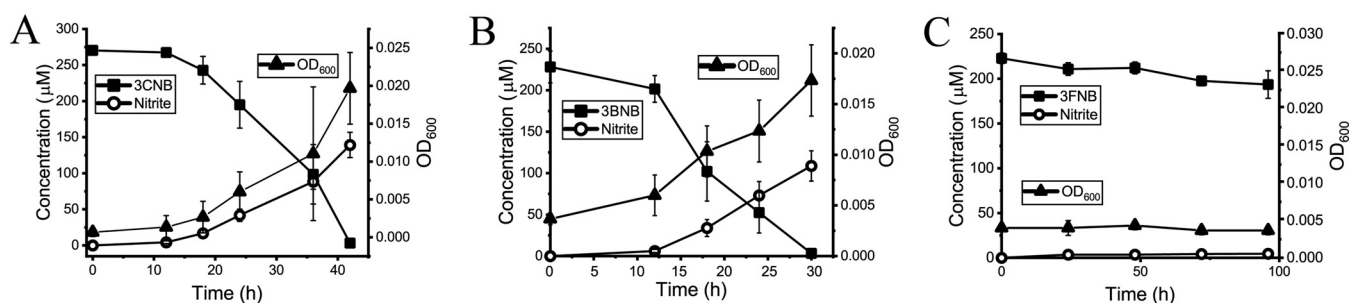


FIG 1 Growth of *Diaphorobacter* sp. strain JS3051 in mineral salts medium (pH 7.0) supplemented with 3CNB (A), 3BNB (B), and 3FNB (C) as sole carbon, nitrogen, and energy sources. Utilization of substrates (■) was analyzed by HPLC. Growth was monitored by measuring absorbance at 600 nm (▲). Nitrite concentration (○) was measured as described in Materials and Methods.

comparable activities toward 3BNB (5.7 nmol/min/mg protein) and 3CNB (5.6 nmol/min/mg protein), but a much reduced activity (1.2 nmol/min/mg protein) toward 3FNB (Fig. 2).

Although the activity of DcbAaAbAcAd in oxidative denitration of 3CNB, 3BNB, and 3FNB is indicated by nitrite release, there are alternative ways for the initial dioxygenation of 3-halogenated nitrobenzenes, i.e., attack at the 1,2- position or 1,6- position, which would produce 3-halogenated catechol or 4-halogenated catechol. GC-MS analysis of the transformation product of 3CNB revealed a product peak at the retention time of 17.63 min with mass spectrum corresponding to the 4-chlorocatechol (Fig. 3A), and no 3-chlorocatechol was detected. Similarly, only 4-bromocatechol was detected from 3-bromonitrobenzene (Fig. 3B). For 3FNB, both 3- and 4-fluorocatechols are produced (Fig. 3C) in a ratio of 1:9 (Table 1), indicating a less rigid product regioselectivity of DcbAaAbAcAd for 3FNB.

Substrate specificity of DcbAc mutants with *meta*-halonitrobenzenes. The 23DCNB dioxygenase (DcbAaAbAcAd) consists of a reductase (DcbAa), a ferredoxin protein, (DcbAb) and an oxygenase (DcbAcAd). Here, the active site residues of the alpha subunit (DcbAc), which determines the substrate specificity (16), were analyzed based on the structure model of DcbAc (13), and the contribution of these residues in controlling the activities and substrate specificity toward *meta*-halonitrobenzenes was evaluated. The E204I mutation (13) caused a significant decrease ($\sim 90\%$) of the activities toward 3CNB and 3BNB with an unchanged product regioselectivity (Fig. 2, Table 1). The mutant showed almost equal activities toward 3CNB, 3BNB, and 3FNB (Fig. 2). When the glutamic acid at position 204 was substituted with aspartic acid, the activities of E204D toward 3CNB and 3BNB (0.9 and 0.8 U/mg protein, respectively) were approximately half that of the wild type (Fig. 2). Neither nitrite nor GC-MS detectable

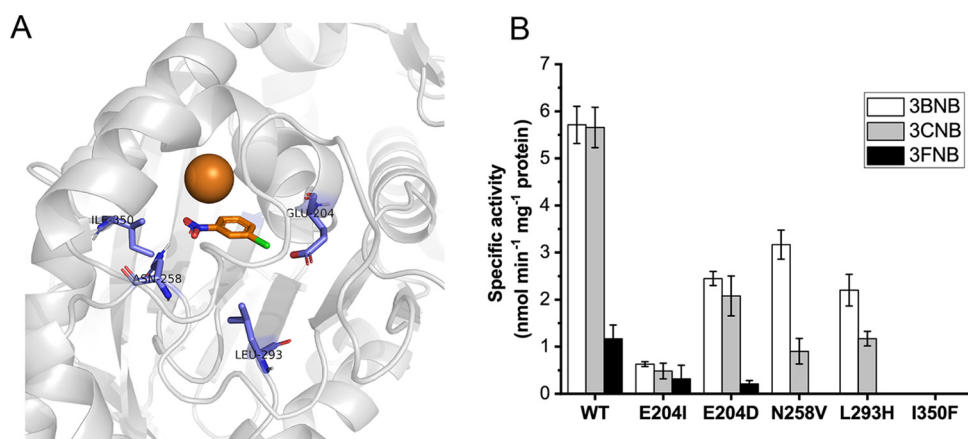


FIG 2 Activity analysis of the active site mutants of DcbAc. (A) The structural model of the active site of DcbAc with 3CNB. The active site residues analyzed in this study are represented in violet color. The mononuclear iron and 3CNB are shown in orange. (B) The activities of DcbAaAbAcAd and its variants toward 3CNB, 3BNB, and 3FNB. Specific activity was measured based on nitrite release, and one unit of enzyme activity is defined as the amount of protein (mg) required for the production of one nmol of nitrite per min.

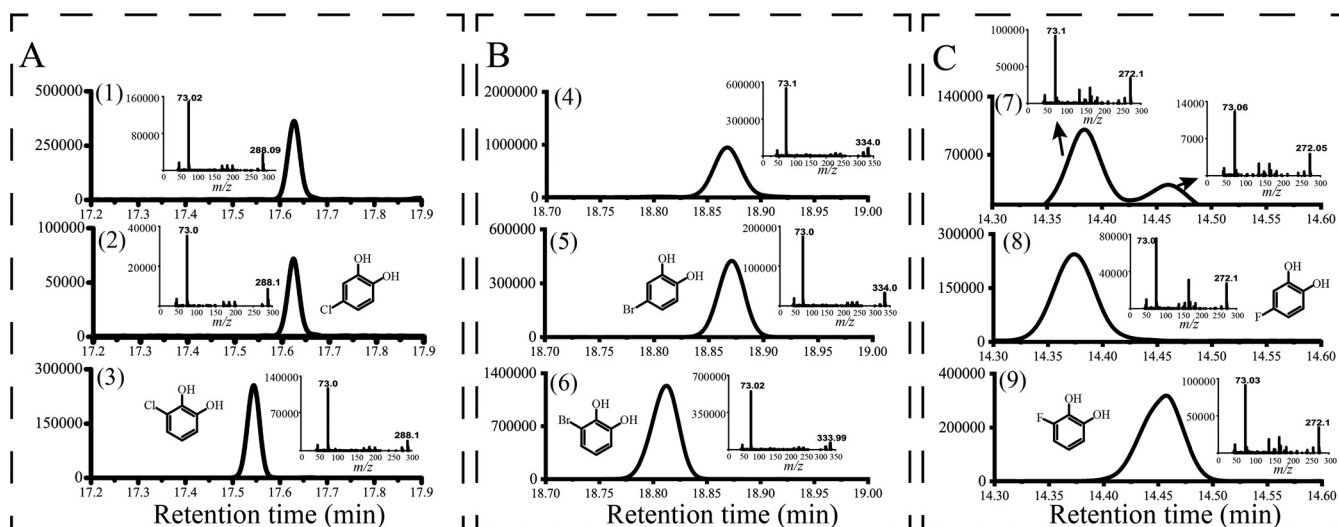


FIG 3 GC-MS analysis of the biotransformation products of halonitrobenzenes by *E. coli* cells carrying the pETDuet-DCB. Panel A: identification of the product from 3CNB. (1) The biotransformation product of 3CNB; (2) authentic 4-chlorocatechol; (3) authentic 3-chlorocatechol. Panel B: identification of the product from 3BNB. (4) The biotransformation product of 3BNB; (5) authentic 4-bromocatechol; (6) authentic 3-bromocatechol. Panel C: identification of the products from 3FNB. (7) The biotransformation products of 3FNB; (8) authentic 4-fluorocatechol; (9) authentic 3-fluorocatechol.

products were produced by the I350F mutant, indicating it is unable to oxidize the *meta*-HNBs.

The N258V and L293H mutants showed decreased rates of nitrite release toward the three analogues (Fig. 2). It was reported previously that the F293H mutation changed the regioselectivity of nitrobenzene dioxygenase (NBDO) from *Comamonas* sp. strain JS765, resulting in a shift from production of 4CC to 3CC from 3CNB (15). In contrast, the L293H mutation had no effect on the regioselectivity of DcbAaAbAcAd in this study (Table 1). The N258V mutation caused a change in the product spectrum of all three substrates. With 3CNB and 3BNB as substrates, the major products produced by the N258V mutant are 4-chloro- or 4-bromocatechol,

TABLE 1 Relative ratios of products produced from HNBS by wild-type DcbAaAbAcAd and its mutants^a

Substrates	Dioxygenases	Catechols produced (% of total products)		
		4CC	3CC	4NCAT
3CNB	WT	100	-	-
	E204D	100	-	-
	E204I	100	-	-
	N258V	66 ± 0.8	-	34 ± 0.8
	L293H	100	-	-
	I350F	-	-	-
3BNB	WT	4BC	3BC	4NCAT
	E204D	100	-	-
	E204I	100	-	-
	N258V	77 ± 0.5	-	23 ± 0.5
	L293H	100	-	-
	I350F	-	-	-
3FNB	WT	92 ± 1.2	8 ± 1.2	-
	E204D	72 ± 1	18 ± 1	-
	E204I	-	-	-
	N258V	-	-	100
	L293H	-	-	-
	I350F	-	-	-

^a3CNB, 3-chloronitrobenzene; 3BNB, 3-bromonitrobenzene; 3FNB, 3-fluoronitrobenzene; 3CC, 3-chlorocatechol; 4CC, 4-chlorocatechol; 3BC, 3-bromocatechol; 4BC, 4-bromocatechol; 3FC, 3-fluorocatechol; 4FC, 4-fluorocatechol; 4NCAT, 4-nitrocatechol; -, none detected.

TABLE 2 Kinetic parameters of DccA for halocatechols derived from *meta*-halogenated nitrobenzene

Substrates	K_m (μM)	V_{max} ($\mu\text{M}/\text{min}$)	K_{cat} (min^{-1})	K_{cat}/K_m ($\text{min}^{-1}\mu\text{M}^{-1}$)
3CC	2.21 ± 0.58	0.29 ± 0.01	11.8	5.3
4CC	0.69 ± 0.14	0.43 ± 0.07	17.4	25.2
3BC	1.03 ± 0.32	0.13 ± 0.04	5.3	5.2
4BC	1.08 ± 0.33	0.47 ± 0.05	18.9	17.5
3FC	2.71 ± 0.21	0.05 ± 0.01	2.0	0.6
4FC	6.73 ± 1.02	0.12 ± 0.05	4.9	0.7

respectively, along with small amounts of 4-nitrocatechol (Table 1). The N258V mutant produced a higher ratio of 4-nitrocatechol from 3CNB (34%) than 3BNB (23%) and did not transform 3FNB (Table 1, Fig. 2).

The activities of chlorocatechol 1,2-dioxygenase (DccA) and chloromuconate cycloisomerase (DccB). The pathway for catabolism of 3CNB and 3BNB in strain JS3051 were predicted based on the modified *ortho*-cleavage pathway for degradation of halocatechols. We hypothesized that strain JS3051 uses the same enzymes for degradation of 3CNB that is used for 23DCNB. DccA from strain JS3051 is a chlorocatechol 1,2-dioxygenase with broad-substrate specificity (13). Its substrate specificity for the halogenated catechols was examined by comparing the kinetic parameters (Table 2). In general, DccA shows a preference for chloro- and bromocatechols (K_{cat}/K_m of $5.2\text{--}25.2 \mu\text{M}^{-1} \text{min}^{-1}$) over fluorocatechols (K_{cat}/K_m of $0.6\text{--}0.7 \mu\text{M}^{-1} \text{min}^{-1}$) (Table 2). In particular, DccA had higher turnover rates and catalytic efficiencies for the 4-chlorocatechol and 4-bromocatechol compared with the respective 3-substituted catechols. The higher K_m values for 3- and 4-fluorocatechols (2.7 and 6.7 μM , respectively) indicated that fluorosubstitution would cause the ring-fission step to be a bottleneck for a 3FNB catabolic pathway.

A coupled enzyme assay with halocatechols as initial substrates was used to test the activities of the chloromuconate cycloisomerase (DccB) toward halogenated muconic acids. With the exception of 2-fluoromuconic acid (produced from 3-fluorocatechol), all tested muconic acid derivatives proved to be substrates of DccB (Fig. 4). The results support the hypothesis that DccB serves as a functional chloromuconate cycloisomerase in the 3CNB and 3BNB catabolic pathway.

DISCUSSION

The results presented here establish the growth of strain JS3051 on 3CNB and 3BNB. The fact that *dcb*- and *dcc*-encoded enzymes catalyzed the key reactions for degradation of all three compounds supports the conclusion that the same set of enzymes is used for catabolism of 3CNB, 3BNB, and 23DCNB via the proposed pathway (Fig. 5). The results strongly support the proposed pathway, but knockouts would be required to conclusively exclude the possibility that other not-yet-identified enzymes are also involved in the degradation of the compounds.

The initial dioxygenase (DcbAaAbAcAd) of strain JS3051 exhibits a higher activity toward 23DCNB than toward 3CNB, whereas the ring-cleavage dioxygenase (DccA) is more efficient for 4-chlorocatechol than for 3,4-dichlorocatechol, the intermediate in the 2,3DCNB catabolic pathway (13). The 4-chlorocatechol catabolic pathway, the lower degradation pathway for 3CNB in this study, has been implicated in degradation of natural chlorinated aromatics such as chlorobenzoic acid (17). The *dcc* genes are highly similar to the *clc* genes that are responsible for the catabolism of 4-chlorocatechol, but not 3,4-dichlorocatechol, in *Pseudomonas knackmussii* B13 (18). Thus, the accommodation of 3CNB as a substrate by the initial dioxygenase might have been the key step in the assembly of the catabolic pathway.

The DcbAc of JS3051 falls into a clade of Rieske iron dioxygenases exhibiting activities toward various nitroaromatic compounds (13). Consistent with these nitroarene dioxygenases, the active site residues at positions of 350, 293, and 258 contributed significantly to the substrate specificity of DcbAc for 3-halogenated nitrobenzene. The altered regiospecificity of the N258V variant of DcbAaAbAcAd toward 3-halogenated nitrobenzene is likely due to the disruption of hydrogen bonding between the Asp258 and the nitro- group, as observed in

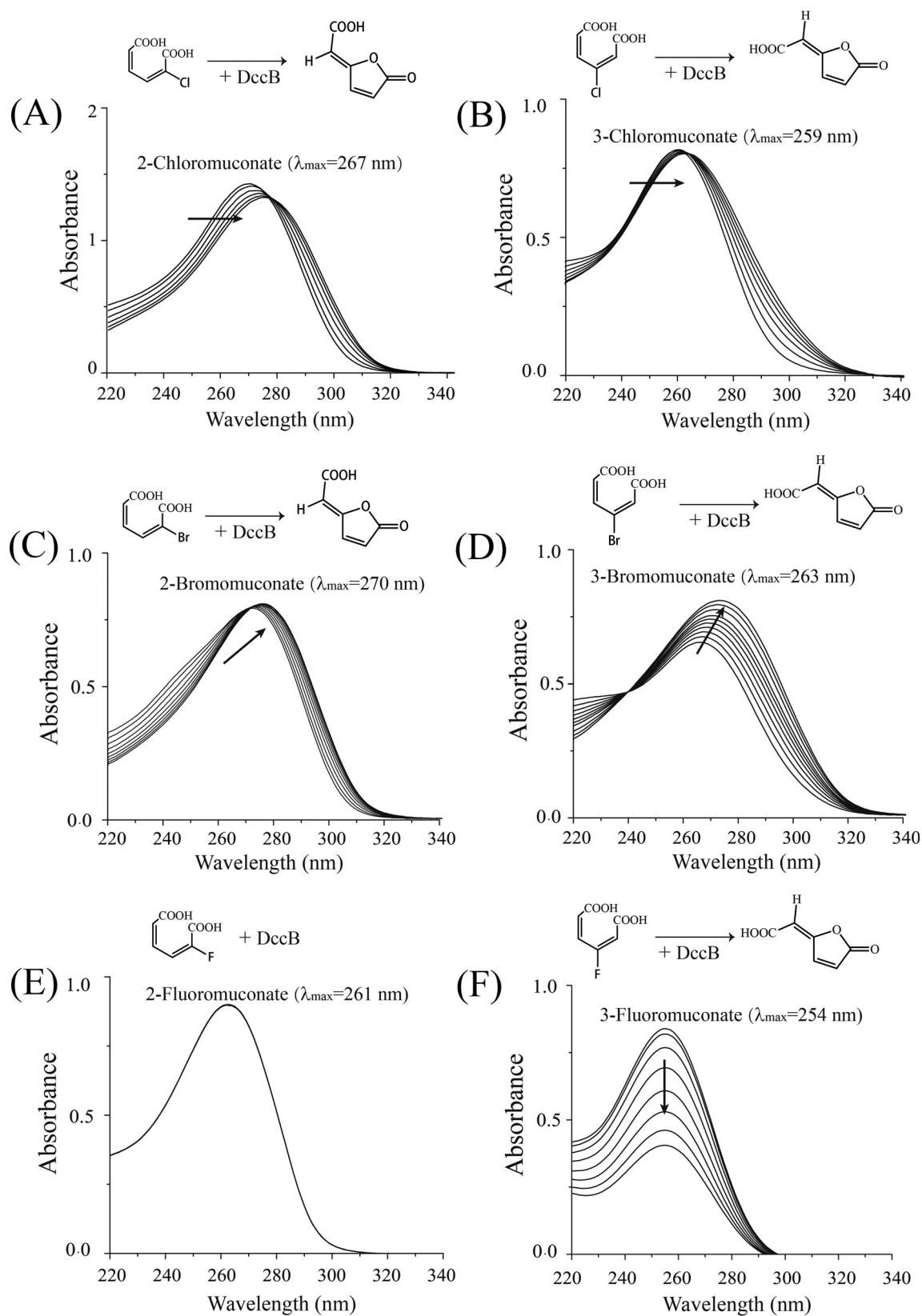


FIG 4 Activities of DccB toward halogenated muconic acids. The reaction mixture (500 μ L) contains 30 μ g of crude enzyme and Tris-HCl buffer (pH 8.0, 50 mM); halocatechols (50 μ M final) were added into the mixtures to initiate the reaction. The halocatechols were first converted to halomuconates by DccA, resulting in an increase of the absorbance at \sim 260 nm. DccB catalyzed the subsequent
(Continued on next page)

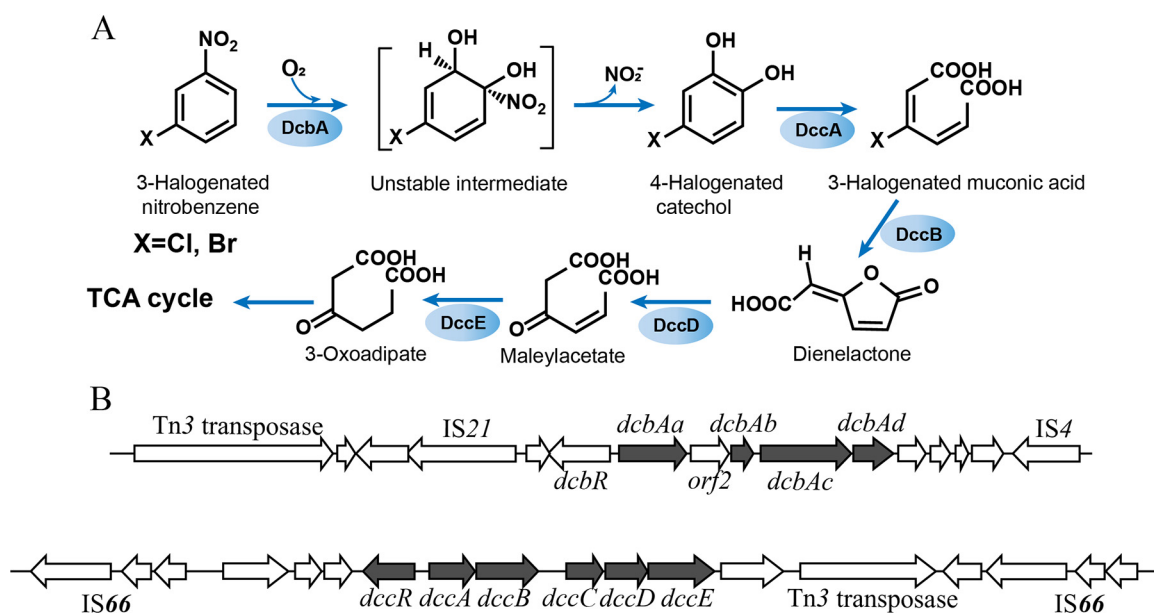


FIG 5 (A) Proposed catabolic pathways of 3CNB and 3BNB in strain JS3051. The activities of DcbA, DccA, and DccB were detected in this study. The reactions catalyzed by DccD (dienelactone hydrolase) and DccE (maleylacetate reductase) are proposed based on the lower catabolic pathway of chlorobenzoate degradation in *Pseudomonas knackmussii* B13 (18), and the amino acid sequences of DccD and DccE are identical to those of ClcD_{B13} and ClcE_{B13}, respectively. (B) The organization of *dcb* and *dcc* gene clusters (13).

nitrobenzene dioxygenase (NBDO) (15, 19, 20). The key difference between DcbAaAbAcAd and other nitroarene dioxygenases is the participation of the glutamic acid residue at position 204 in halogen binding. The *meta*-halogen atom of 3-chloronitrobenzene is predicted to form a halogen bond with the nucleophilic carbonyl group of Glu 204 (Fig. 2A). Aromatic compounds with halogen substituents are expected to have a strong positive σ -hole ($I > Br > Cl$), but fluorine fails to form a positive σ -hole due to its higher electronegativity (21, 22). This is consistent with the lower activity of DcbAaAbAcAd toward 3FNB than 3CNB and 3BNB. In addition, the lack of halogen binding to stabilize the 3FNB in the active pocket would explain the less rigid product regioselectivity of DcbAaAbAcAd with 3FNB than with 3CNB and 3BNB (Table 1).

Biodegradation of fluorosubstituted aromatics was widely observed (23), whereas in some cases, bacteria could grow on chloro- and bromo-substituted aromatic compounds but not on the corresponding fluorinated analogues. For example, *Pseudomonas stutzeri* ZWLR2-1 could grow on 2-chloronitrobenzene and 2-bromonitrobenzene but not on 2-fluoronitrobenzene (7). *Pseudomonas knackmussii* B13 uses 3-chloro- and 3-bromobenzoate, but not 3-fluorobenzoate, as sole sources of carbon and energy (24, 25). The molecular details for biodegradation of 2-chloro/bromonitrobenzene and 3-chloro/bromobenzoate in strains ZWLR2-1 and B13 were elucidated, whereas the factors that cause the bacteria to be unable to utilize corresponding fluorinated analogues are little understood. In the present study, several lines of evidence indicate that both the initial dioxygenase and the lower pathway enzymes obstructed the catabolic flux of 3FNB but not that of 3CNB and 3BNB in strain JS3051 as follows. (i) The DcbAaAbAcAd exhibits a lower activity toward 3FNB than 3CNB or 3BNB (Fig. 2). Moreover, the low degree of regioselectivity of DcbAaAbAcAd for 3FNB would result in the formation of both 3-fluorocatechol and 4-fluorocatechol as intermediates (Table 1), which might misroute

FIG 4 Legend (Continued)

lactonization of the halomuconates. The spectra shown were recorded at 30 s intervals for corresponding halogenated muconic acids from 3-chlorocatechol (A), 4-chlorocatechol (B), 3-bromocatechol (C) and 4-bromocatechol (D), and 160 s for 3-fluorocatechol (E) and 4-fluorocatechol (F), after the maximum absorbance at 260 nm was obtained. No spectral change was observed for 2-fluoromuconate in the presence of DccB (E).

TABLE 3 Strains and plasmids used in this study

Strains and plasmids	Description	Source
Strains		
<i>Diaphorobacter</i> sp. strain JS3051	2,3-dichloronitrobenzene utilizer	9
<i>E. coli</i> strains DH5 α	<i>supE44 lacU169</i> (ϕ 80d <i>lacZ</i> Δ M15) <i>recA1 endA1 hsdR17 thi-1 gyrA96 relA1</i>	Novagen
<i>E. coli</i> BL21(DE3)	F- <i>ompT hsdS_B(r_B- m_B-)</i> <i>gal dcm lacY1</i> (DE3)	Novagen
Plasmids		
pET28-28a(+)	IPTG inducible expression vector, Kan ^r	Novagen
pETDuet-1	IPTG inducible coexpression vector, Amp ^r	Novagen
pET- <i>dccA</i>	<i>dccA</i> fragment inserted into pET-28a(+) between <i>NdeI</i> and <i>BamHI</i> ; Kana ^r	13
pET- <i>dccAB</i>	<i>dccAB</i> fragment inserted into pET-28a(+) between <i>NdeI</i> and <i>BamHI</i> ; Kana ^r	13
pETDuet-DCB	<i>NcoI-SacI</i> fragment containing <i>dcbAaAb</i> and <i>NdeI-KpnI</i> fragment containing <i>dcbAcAd</i> inserted into pETDuet-1; Amp ^r	13

the catabolic pathway and reduce its effectiveness. (ii) For the ring-cleavage step, DccA has the highest catalytic efficiencies for 4-chlorocatechol and 4-bromocatechol, which are the products from dioxygenation of 3CNB and 4CNB, whereas the catalytic efficiencies of DccA for 3-fluorocatechol and 4-fluorocatechol are 10- to 90-fold lower than those of their chloro- and bromo- analogues (Table 1). (iii) DccB is unable to catalyze the lactonization of 2-fluoromuconic acid, which is the ring-cleavage product of 3-fluorocatechol (Fig. 4). The production of a small amount of 3-fluorocatechol from 3FNB by DcbAaAbAcAd (Table 1) would then result in accumulation of 2-fluoromuconic as a dead-end product in strain JS3051.

Strain JS3051 showed robust growth on 3CNB, and its doubling time is about half that of the metabolically engineered 3CNB degrader in which the catabolic genes were not substrate-inducible (15). In contrast, our preliminary induction assays based on the β -galactosidase activity suggested that DcbR is able to respond to 3CNB, 3BNB as well as 3FNB (data not shown). The tightly controlled expression of the catabolic genes in strain JS3051 (9, 13) might be a factor contributing to its robust growth on 3CNB. The putative LysR-family regulator DcbR next to Dcb-encoding genes is identical to the NtdR from the 2-nitrotoluene utilizer *Acidovorax* sp. JS42, and the sequence of the *dcb* promoter region is also identical to that of *ntd*. NtdR, the activator of *ntd* genes, was reported to respond to a wide range of nitroaromatic compounds including nitrotoluenes, chloronitrobenzenes, 2,4-dinitrotoluene, and 1-nitronaphthalene (26). Although it seems that the DcbR is also a broad substrate regulator similar to NtdR, it is unclear whether the expression level under different inducers has an impact on the growth capacity of strain JS3051 on these substrates.

MATERIALS AND METHODS

Chemicals, strains, and plasmids. All chemicals were obtained from Sigma (St. Louis, MO) with the following exceptions: 3-chlorocatechol (TCI, Japan), 4-bromocatechol, 3-bromocatechol, 4-fluorocatechol, and 4-nitrocatechol (Bide Pharm, China), and 3-fluorocatechol (Accela, China). Strains and plasmids used in this study are listed in Table 3. *E. coli* strains were cultured at 37°C in lysogeny broth (LB). Antibiotics (40 μ g/mL kanamycin or 100 μ g/mL ampicillin) were supplemented as necessary. *Diaphorobacter* sp. strain JS3051 was grown in minimal salts medium (MSM) (6) with *meta*-halonitrobenzenes (~0.2 mM) or glucose (2 mM) at 30°C. MSM (pH 7.0) contains 14.3 g of Na₂HPO₄·12H₂O, 3 g of KH₂PO₄, 1 mg of CaCl₂, 0.28 mg of MnSO₄·H₂O, 0.05 mg of ZnSO₄, 0.3 mg of FeSO₄·7H₂O, 0.06 mg of MgSO₄·7H₂O, 0.05 mg of CuSO₄, and 0.05 mg of H₃BO₃ per liter of deionized water.

Growth of strain JS3051. The ability of strain JS3051 to grow on 3CNB, 3BNB, or 3FNB was tested in MSM under aerobic conditions. It was first cultured in 10 mL of MSM containing 23DCNB (200 μ M) and yeast extract (0.001%) to stationary phase. The cells were collected by centrifugation (7000 \times g, 5 min) and washed twice with MSM, then resuspended in 5 mL of MSM as seed culture. Growth assays were conducted in 50 mL of MSM supplemented with various substrates at final concentrations of 200–300 μ M. The concentrations of substrates and nitrite as well as the optical density at 600 nm (OD₆₀₀) were measured at appropriate intervals.

Biotransformation assays. 23DCNB dioxygenase was heterologously expressed with the pETDuet-DCB containing *dcbAaAbAcAd* (GenBank accession numbers: QPN31022.1, QPN31023.1, QPN31024.1, and QPN31025.1) in *E. coli* as previously reported (13). *E. coli* strain BL21(DE3) (pETDuet-DCB) was inoculated into 150 mL of LB medium containing 100 μ g mL⁻¹ ampicillin and grown at 37°C until optical density at 600 nm (OD₆₀₀) reached 0.6. Induction of gene expression was conducted by adding 0.3 mM isopropyl- β -D-thiogalactopyranoside (IPTG) and the cells were grown for an extra 12 h at 16°C. The cells were harvested by centrifugation (7000 \times g, 10 min, 4°C) and washed twice with Tris-HCl buffer (pH 7.4, 50 mM). Whole cell biotransformation was conducted using reaction mixtures with a cell density (OD₆₀₀) of 2 and appropriate substrates at

TABLE 4 Oligonucleotide primers used for site-directed mutagenesis

Oligonucleotides	Sequences(5'–3')	Description
DCBE204D-F	AACTTCGTTGGTGACGATTACCACGTTGGTTGGAC	pETDuet-DCB204
DCBE204D-R	GTCCAACCAACGTGGAATCGTCACCAACGAAGTT	
DCBE204I-F	GGTCCAACCAACGTGGTATATGTCACCAACGAAGTTTTCA	pETDuet-DCB204
DCBE204I-R	TGAAAACCTCGTTGGTGACATATACCACGTTGGTTGGACC	
DCBN258V-F	GGGACTACTACGCTGGTGTCTTCTCTGCTGACATGG	pETDuet-DCB258
DCBN258V-R	CCATGTCAGCAGAGAAGACACCAGCGTAGTAGTCCC	
DCBL293H-F	GCTCGTATCTACCGTTTCATCTGAACGGTACTGTTTTCC	pETDuet-DCB293
DCBL293H-R	GGAAAACAGTACCGTTTCAGATGAGAACGGTAGATACGAGC	
DCBI350F-F	TGACGCTGTTACGCGTCTTTCGGTCCGGC	pETDuet-DCB350
DCBI350F-R	GCCGGACCGAAAGAACGCTGAACAGCGTCA	

30°C under aerobic conditions, with sampling at appropriate intervals for analyses of the substrates and products. All reactions were performed in triplicate. The Griess method was used to detect nitrite (27). Protein concentrations were measured with an enhanced BCA protein assay kit (Beyotime Biotechnology Shanghai, China). Biotransformation assays for the 23DCNBDO variants were performed in the same way.

Site-directed mutagenesis. The structural model of DcbAc complexed with 3CNB was generated using a described method (13). Site-directed mutagenesis of *dcbAc* was performed by PCR with the primers listed in Table 4, using pETDuet-DCB as a template (13). The program was 95°C for 5 min, 95°C for 30s, 58°C for 15s, 72°C for 8 min for 30 cycles, followed by 5 min at 72°C. The mutation sites were identified by sequencing. The resultant plasmids were transformed into *E. coli* strain BL21(DE3) for protein expression.

Enzyme assays. The 1,2-chlorocatechol dioxygenase DccA (GenBank accession number: [OPN32561.1](#)) was expressed and purified as described previously (13). Total reaction volume was 500 μ L, containing 0.53 μ g of DccA with 50 mM Tris-HCl (pH 8.0) and 0.5–150 μ M halogenated catechols. The reactions for the conversion of halogenated catechols into muconic acids were monitored by the linear increase in absorbance at A_{260} with a Lambda 25 spectrophotometer (Perkin Elmer/Cetus, Norwalk, CT). The observed rates were fit to the Michaelis-Menten equation to obtain the steady-state rate constants. The molar extinction coefficients for halogenated muconic acids at 260 nm were as described by Dorn and Knackmuss (28): 17,100 $M^{-1}cm^{-1}$ for 2-chloromuconic acid; 12,400 $M^{-1}cm^{-1}$ for 3-chloromuconic acid; 14,400 $M^{-1}cm^{-1}$ for 2-bromomuconic acid; 7,900 $M^{-1}cm^{-1}$ for 3-bromomuconic acid; and 14,900 $M^{-1}cm^{-1}$ for 2- and 3-fluoromuconic acid.

A coupled enzyme assay was used to detect the activity of chloromuconate cycloisomerase toward halogenated muconic acids. DccA (1,2-chlorocatechol dioxygenase) and DccB (chloromuconate cycloisomerase) were coexpressed in *E. coli* cells carrying pET-*dccAB* (13). Protein expression and preparation of the crude enzyme were as described previously (13). The reaction mixture contained 30 μ g of crude enzyme in 499 μ L of Tris-HCl buffer (pH 8.0, 50 mM); halocatechols (50 μ M) were added into the mixture to initiate the reactions. The activity of chloromuconate cycloisomerase was monitored by scanning the absorption spectra from 200 to 400 nm at appropriate intervals with a Lambda 25 spectrophotometer (PerkinElmer/Cetus, Norwalk, CT).

Analytical methods. The products from whole-cell biotransformation were extracted with equal volumes of ethyl acetate. The solvent was evaporated and the residue dissolved in 0.05 mL of anhydrous acetonitrile, then derivatized by adding equal volumes of *N,O*-bis(trimethylsilyl)trifluoroacetamide (BSTFA) at 70°C for 35 min. The resultant products were identified by gas chromatography-mass spectrometry (GC-7890B MS-5977B, Agilent, USA) under the following conditions: HP-5MS column (30 m \times 0.25 mm \times 0.25 μ m, Agilent, USA), interface temperature 290°C, source temperature 230°C. Column temperature program: initial temperature 70°C for 2 min, raised to 130°C at 5°C/min, increased to 180°C at 10°C/min, increased to 285°C at 5°C/min, holding for 1 min. Mass spectrometer conditions: 33–750 *m/z* mass range at the electron energy of 70 eV, EI energy source. HPLC was performed using a Waters e2695 chromatograph with a Waters 2998 photo diode array detector and a C_{18} reversed-phase column (250 by 4.6 mm) (Agilent, USA). The mobile phase was water containing 0.1% (vol/vol) acetic acid (solution A) and methanol (solution B). The gradient was 0–5 min, 20% (vol/vol) B; 5–20 min, 20–90% B linear; 20–25 min, 90% B.

Data availability. No new gene or protein sequence was produced in this study. The GenBank accession numbers of all genes mentioned in this study are listed in the text.

ACKNOWLEDGMENTS

This work was supported by grants from the National Key R&D Program of China (2021YFA0909500), National Natural Science Foundation of China (NSFC) (31900075 and 31870084), and DuPont Corporate Remediation Group (contract LBIO-65019).

This work does not include any human or animal materials.

We declare no conflict of interest.

REFERENCES

- Booth G. 2012. Nitro compounds, aromatic. In Ullmann's encyclopedia of industrial chemistry. WileyVCH Verlag GmbH & Co KGaA, Weinheim, Germany.
- International Agency for Research on Cancer. 1996. 2-chloronitrobenzene, 3-chloronitrobenzene and 4-chloronitrobenzene. IARC Monogr Eval Carcinog Risks Hum 65:263–296.

3. Yurawecz MP, Puma BJ. 1983. Identification of chlorinated nitrobenzene residues in Mississippi River fish. *J Assoc off Anal Chem* 66:1345–1352. <https://doi.org/10.1093/jaoac/66.6.1345>.
4. Feltes J, Levens K, Volmer D, Spiekermann M. 1990. Gas chromatographic and mass spectrometric determination of nitroaromatics in water. *J Chromatogr* 518:21–40. [https://doi.org/10.1016/S0021-9673\(01\)93159-0](https://doi.org/10.1016/S0021-9673(01)93159-0).
5. National Center for Biotechnology Information. 2022. PubChem annotation record for 1-chloro-3-nitrobenzene. Hazardous Substances Data Bank (HSDB). <https://pubchem.ncbi.nlm.nih.gov/source/hsdb/1323>. Accessed 1 October 2021.
6. Liu H, Wang SJ, Zhou NY. 2005. A new isolate of *Pseudomonas stutzeri* that degrades 2-chloronitrobenzene. *Biotechnol Lett* 27:275–278. <https://doi.org/10.1007/s10529-004-8293-3>.
7. Wang L, Gao YZ, Zhao H, Xu Y, Zhou NY. 2019. Biodegradation of 2-bromonitrobenzene by *Pseudomonas stutzeri* ZWLR2-1. *Int Biodeterior Biodegradation* 138:87–91. <https://doi.org/10.1016/j.ibiod.2018.12.008>.
8. Zhen D, Liu H, Wang SJ, Zhang JJ, Zhao F, Zhou NY. 2006. Plasmid-mediated degradation of 4-chloronitrobenzene by newly isolated *Pseudomonas putida* strain ZWL73. *Appl Microbiol Biotechnol* 72:797–803. <https://doi.org/10.1007/s00253-006-0345-2>.
9. Palatucci ML, Waidner LA, Mack EE, Spain JC. 2019. Aerobic biodegradation of 2,3- and 3,4-dichloronitrobenzene. *J Hazard Mater* 378:120717. <https://doi.org/10.1016/j.jhazmat.2019.05.110>.
10. Wu JF, Jiang CY, Wang BJ, Ma YF, Liu ZP, Liu SJ. 2006. Novel partial reductive pathway for 4-chloronitrobenzene and nitrobenzene degradation in *Comamonas* sp. strain CNB-1. *Appl Environ Microbiol* 72:1759–1765. <https://doi.org/10.1128/AEM.72.3.1759-1765.2006>.
11. Liu H, Wang SJ, Zhang JJ, Dai H, Tang H, Zhou NY. 2011. Patchwork assembly of *nag*-like nitroarene dioxygenase genes and the 3-chlorocatechol degradation cluster for evolution of the 2-chloronitrobenzene catabolism pathway in *Pseudomonas stutzeri* ZWLR2-1. *Appl Environ Microbiol* 77:4547–4552. <https://doi.org/10.1128/AEM.02543-10>.
12. Gao YZ, Palatucci ML, Waidner LA, Li T, Guo Y, Spain JC, Zhou NY. 2021. A *Nag*-like dioxygenase initiates 3,4-dichloronitrobenzene degradation via 4,5-dichlorocatechol in *Diaphorobacter* sp. strain JS3050. *Environ Microbiol* 23:1053–1065. <https://doi.org/10.1111/1462-2920.15295>.
13. Li T, Gao YZ, Xu J, Zhang ST, Guo Y, Spain JC, Zhou NY. 2021. A recently assembled degradation pathway for 2,3-dichloronitrobenzene in *Diaphorobacter* sp. strain JS3051. *mBio* 12:e0223121. <https://doi.org/10.1128/mBio.02231-21>.
14. Park HS, Lim SJ, Chang YK, Livingston AG, Kim HS. 1999. Degradation of chloronitrobenzenes by a coculture of *Pseudomonas putida* and a *Rhodococcus* sp. *Appl Environ Microbiol* 65:1083–1091. <https://doi.org/10.1128/AEM.65.3.1083-1091.1999>.
15. Ju KS, Parales RE. 2009. Application of nitroarene dioxygenases in the design of novel strains that degrade chloronitrobenzenes. *Microb Biotechnol* 2:241–252. <https://doi.org/10.1111/j.1751-7915.2008.00083.x>.
16. Parales JV, Parales RE, Resnick SM, Gibson DT. 1998. Enzyme specificity of 2-nitrotoluene 2,3-dioxygenase from *Pseudomonas* sp. strain JS42 is determined by the C-terminal region of the alpha subunit of the oxygenase component. *J Bacteriol* 180:1194–1199. <https://doi.org/10.1128/JB.180.5.1194-1199.1998>.
17. Ogawa N, Miyashita K, Chakrabarty AM. 2003. Microbial genes and enzymes in the degradation of chlorinated compounds. *Chem Rec* 3:158–171. <https://doi.org/10.1002/tcr.10059>.
18. Gaillard M, Vallaes T, Vorholter FJ, Minoia M, Werlen C, Sentchilo V, Puhler A, van der Meer JR. 2006. The *clc* element of *Pseudomonas* sp. strain B13, a genomic island with various catabolic properties. *J Bacteriol* 188:1999–2013. <https://doi.org/10.1128/JB.188.5.1999-2013.2006>.
19. Friemann R, Ivkovic-Jensen MM, Lessner DJ, Yu CL, Gibson DT, Parales RE, Eklund H, Ramaswamy S. 2005. Structural insight into the dioxygenation of nitroarene compounds: the crystal structure of nitrobenzene dioxygenase. *J Mol Biol* 348:1139–1151. <https://doi.org/10.1016/j.jmb.2005.03.052>.
20. Ju KS, Parales RE. 2006. Control of substrate specificity by active-site residues in nitrobenzene dioxygenase. *Appl Environ Microbiol* 72:1817–1824. <https://doi.org/10.1128/AEM.72.3.1817-1824.2006>.
21. Auffinger P, Hays FA, Westhof E, Ho PS. 2004. Halogen bonds in biological molecules. *Proc Natl Acad Sci USA* 101:16789–16794. <https://doi.org/10.1073/pnas.0407607101>.
22. Shinada NK, de Brevern AG, Schmidtke P. 2019. Halogens in protein-ligand binding mechanism: a structural perspective. *J Med Chem* 62:9341–9356. <https://doi.org/10.1021/acs.jmedchem.8b01453>.
23. Kiel M, Engesser KH. 2015. The biodegradation vs. biotransformation of fluorosubstituted aromatics. *Appl Microbiol Biotechnol* 99:7433–7464. <https://doi.org/10.1007/s00253-015-6817-5>.
24. Dorn E, Hellwig M, Reineke W, Knackmuss HJ. 1974. Isolation and characterization of a 3-chlorobenzoate degrading pseudomonad. *Arch Microbiol* 99:61–70. <https://doi.org/10.1007/BF00696222>.
25. Schreiber A, Hellwig M, Dorn E, Reineke W, Knackmuss HJ. 1980. Critical reactions in fluorobenzoic acid degradation by *Pseudomonas* sp. B13. *Appl Environ Microbiol* 39:58–67. <https://doi.org/10.1128/aem.39.1.58-67.1980>.
26. Ju KS, Parales JV, Parales RE. 2009. Reconstructing the evolutionary history of nitrotoluene detection in the transcriptional regulator NtdR. *Mol Microbiol* 74:826–843. <https://doi.org/10.1111/j.1365-2958.2009.06904.x>.
27. Lessner DJ, Johnson GR, Parales RE, Spain JC, Gibson DT. 2002. Molecular characterization and substrate specificity of nitrobenzene dioxygenase from *Comamonas* sp. strain JS765. *Appl Environ Microbiol* 68:634–641. <https://doi.org/10.1128/AEM.68.2.634-641.2002>.
28. Dorn E, Knackmuss HJ. 1978. Chemical structure and biodegradability of halogenated aromatic compounds. Substituent effects on 1,2-dioxygenation of catechol. *Biochem J* 174:85–94. <https://doi.org/10.1042/bj1740085>.